

# Phase transition and soft phonon modes in SrZrO<sub>3</sub> around 1200 °C by ultraviolet laser Raman spectroscopy

Hiroataka Fujimori,\* Masatomo Yashima,† Masato Kakihana, and Masahiro Yoshimura  
Materials and Structures Laboratory, Tokyo Institute of Technology, Yokohama, 226-8503, Japan

(Received 2 June 1999; revised manuscript received 17 August 1999)

Raman spectra of SrZrO<sub>3</sub> have been successfully obtained at temperatures from 600 °C to 1240 °C by using a new continuous-wave ultraviolet Raman spectroscopic system. The phase transition between cubic and tetragonal phases is due to the collapse of the  $R_{25}$  mode at the  $R$  point of the high-temperature cubic Brillouin zone. Two phonon modes observed to soften (decrease) in frequency approach together and their peak intensities continuously decreased with increasing temperature. They disappeared between 1200 °C and 1220 °C. The soft modes remain underdamped, the damping constant of soft modes increased with temperature toward phase-transition temperature satisfying the universal scaling law.

## I. INTRODUCTION

It has been known that SrZrO<sub>3</sub>-based oxides exhibited an appreciable proton conduction.<sup>1</sup> Their physical and chemical properties relating to such uses strongly depend on the crystal structures. From the point of view of both physical properties and applications, it is of vital importance to study the effect of temperature on structural distortions and phase transitions. SrZrO<sub>3</sub> belongs to the perovskite family with general formula  $A^{2+}B^{4+}O_3$ .<sup>2</sup> A sequence of phase transitions was found by Carlsson<sup>3</sup> using differential thermal analysis and x-ray diffraction. The structures of SrZrO<sub>3</sub> perovskite at 760 °C and 900 °C were determined later by Ahtee<sup>4</sup> using neutron powder profile refinement. The heat capacity and thermal expansion of SrZrO<sub>3</sub> have been determined by Zhao<sup>5</sup> and Ligny.<sup>6</sup> The crystallographic symmetries of SrZrO<sub>3</sub> perovskite at different temperature ranges are shown in Table I, which is a typical sequence of successive and reversible structural phase transitions in centrosymmetric  $ABO_3$  perovskites caused by cooperative  $BO_6$  octahedral tilting.<sup>7-8</sup> The cubic ( $Pm\bar{3}m$ )→tetragonal ( $I4/mcm$ ), tetragonal ( $I4/mcm$ )→orthorhombic ( $Cmcm$ ), and orthorhombic ( $Cmcm$ )→orthorhombic ( $Pbnm$ ) phase transitions have been suggested to be accompanied by the oxygen octahedron antiphase tilt about [001], in-phase tilt about [010], and antiphase tilt about [100] from ideal perovskite structure, respectively.<sup>4</sup> This series of transitions indicates that the sequence of condensation of soft modes from high-temperature cubic phase is  $R_{25}$ ,  $M_3$ , and finally  $R_{25}$  again.<sup>4</sup> However the temperature dependence of soft modes in SrZrO<sub>3</sub> at temperatures higher than 1000 °C was not known yet. One of the major reasons may be caused by the difficulty in recording Raman spectra of materials at high temperatures due to the relatively weak Raman scattering in comparison with the intense, continuous background by thermal emission.

Ultraviolet (UV) Raman spectroscopy is more suitable for measurements at high temperatures, because the UV excitation shifts the wavelengths of Raman scattering away from the peak intensity of the thermal emission to lower wavelength positions. Thus in this study Raman measurements for a SrZrO<sub>3</sub> at various high temperatures have been performed by using a new CW (continuous-wave) ultraviolet (UV) Raman spectroscopic system designed to measure the Raman scattering from materials at high temperature.<sup>9</sup> Moreover we have confirmed that the cubic ( $Pm\bar{3}m$ )→tetragonal ( $I4/mcm$ ) phase transition was triggered by the collapse of the  $R_{25}$  phonon branch at the  $R$  point of the high-temperature Brillouin zone. The study of the soft mode line shape has revealed an unexpected singularity in the damping near the transition temperature. The detailed nature of this phase transition has remained unclear. This study can provide important information for understanding the theoretical model concerning the role played by lattice dynamics in the displacive phase transition.

## II. EXPERIMENTS AND DATA ANALYSIS

### A. Sample preparation

It is important to use compositional homogeneous sample for study of the temperature dependence of soft modes. The polymerized complex method was used to prepare compositional homogeneous sample. Its detail was described elsewhere.<sup>10</sup> Anhydrous citric acid (CA) was added to ethylene glycol (EG) and the CA-EG mixture was stirred at about 100 °C until it became transparent. ZrOCl<sub>2</sub>·8H<sub>2</sub>O and SrCO<sub>3</sub> were dissolved into the CA-EG mixture. The clear solution obtained was heated with stirring up to about 130 °C in order to promote the esterification and gelation between CA and EG. As the solution became concentrated, it became highly viscous indicating the formation of an organic polymeric gel.

TABLE I. Phase transition of SrZrO<sub>3</sub> (Ref. 4).

	700 °C		830 °C		1170 °C	
Orth. ( $Pbnm$ )	— — —	Orth. ( $Cmcm$ )	— — —	Tetra. ( $I4/mcm$ )	— — —	Cubic ( $Pm\bar{3}m$ )
	$R_{25}$		$M_3$		$R_{25}$	

The viscous polymeric product was heat-treated between about 200 °C and 350 °C to remove undesirable solvent and organics. The black powder obtained was calcined in air at about 500 °C for 1 h. It was pressed into pellet, calcined in air at about 1650 °C for 24 h.

### B. An ultraviolet Raman spectroscopic system

Raman measurement for SrZrO<sub>3</sub> specimen at various temperatures has been performed by using a new CW ultraviolet (UV) Raman spectroscopic system designed to measure the Raman scattering from materials at high temperature.<sup>9</sup> This system is based on an ultraviolet argon-ion laser (363.8 nm), a spatial filter, a single monochromator coupled to a double-grating rejection filter, and a two-dimensional charge-coupled device detector. The plasma lines from the laser are rejected by a Pellin-Broca prism combined with apertures. Its detail was described elsewhere.<sup>9</sup> It has been reported that the UV excitation provides good-quality Raman spectra with practically flat backgrounds even at 1500 °C in sharp contrast to the conventional visible excitation in Ref. 9. The sample was mounted in a furnace with a Pt-Rh heater where the sample was placed and then fixed on a Pt/13% Rh thermocouple with alumina cement. The specimen was heated at rate of 10 °C/min, and then temperature was kept constant during the measurements (within  $\pm 1$  °C). Each measurement was done in air after a constant temperature was maintained for 10 min. The laser power at the tube level was set at 200 mW. In consideration of the spectral resolution and high spectral intensity at high temperature, the entrance slit width was set at 100  $\mu\text{m}$ , which corresponds to the full width at half-maximum of 4.7  $\text{cm}^{-1}$ . The Hg line was used for Raman shift calibration for each measurement. No artificial smoothing was used on the acquired Raman spectra.

### III. RESULTS AND DISCUSSION

The powder x-ray diffraction pattern showed the sample that was prepared by the polymerized complex method was orthorhombic single phase<sup>1</sup> at room temperature. In the Raman spectra of 80–200  $\text{cm}^{-1}$  measured with increasing temperatures [Figs. 1(a) and 1(b)], the lines showed a red shift and an increase in line width as the temperature increases. The pattern decomposition of the Raman spectra was performed using a commercial profile-fitting program GRAMS (Fig. 2) and assuming Lorentz functions and intense plasma lines from laser source [\* in Fig. 1(a)]. In the present study, we pay attention to the Raman-inactive triply degenerate  $R_{25}(F_{2u})$  mode in the cubic phase. This is the zone-boundary mode associated with the rotation of the BO<sub>6</sub> octahedra, which is expected to split into Raman-active  $E_g$  and  $A_{1g}$  modes in the tetragonal phase due to out-of-condensation of the  $R_{25}(F_{2u})$  mode. Thus pattern decomposition of the Raman spectra in Fig. 1(a) was performed assuming  $E_g$  and  $A_{1g}$  (Fig. 2). It was impossible to perform the pattern decomposition due to weak Raman intensity in the temperature region from 1100 °C to 1200 °C [Fig. 1(b)]. In Fig. 3, the obtained values of the mode frequencies are plotted as a function of temperature. The optical  $E_g$  and  $A_{1g}$  modes showed remarkable softening approached together and their peak intensities continuously decreased with increasing temperature. They disappeared between 1200 °C and 1220 °C

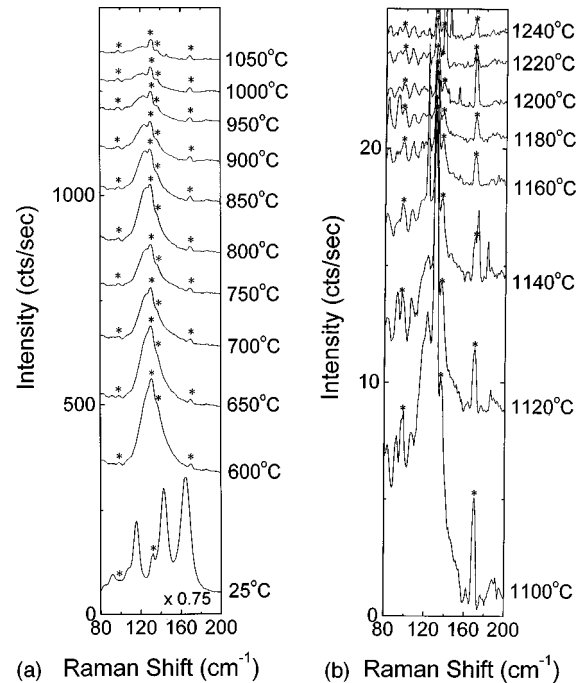


FIG. 1. Temperature dependence of Raman spectra of SrZrO<sub>3</sub> excited by 363.8 nm UV laser line in the region (a) 25–1050 °C, (b) 1100–1240 °C. The plasma lines (\*) from the laser source appeared, because of weak Raman scattering intensity. Note scale factor applied to spectrum at 25 °C.

[Fig. 1(b)], which indicates that Raman-active  $E_g$  and  $A_{1g}$  modes change to Raman-inactive  $R_{25}(F_{2u})$  mode. This result clearly shows that the tetragonal phase ( $I4/mcm$ ) transforms into the cubic phase ( $Pm\bar{3}m$ ) between 1200 °C and 1220 °C, which is consistent with the transition temperature determined by Carlsson<sup>3</sup> and Ligny.<sup>6</sup> The frequency squared  $\omega_0^2$  has a linear relation with temperature and is expressed by

$$\omega_0^2 = \omega_{T_c}^2 + a(T - T_c),$$

where  $\omega_{T_c}^2$  is  $1.29(2) \times 10^4 \text{ cm}^{-2}$ ,  $a$  is  $6.3(6) \text{ cm}^{-2}/\text{K}$  for  $E_g$  mode in the temperature region from 850 °C to 1050 °C. The damping constant of soft modes  $\Gamma$  increased with tempera-

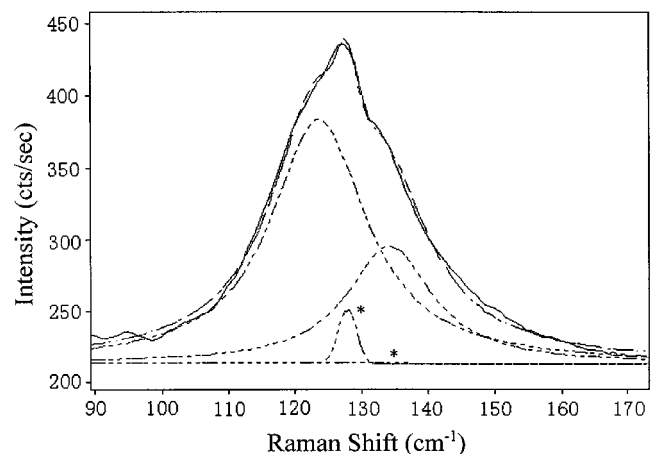


FIG. 2. Pattern decomposition of the Raman spectrum at 600 °C assuming Lorentz functions, which full widths at half maximum were equal, and intense plasma lines from laser source (\*).

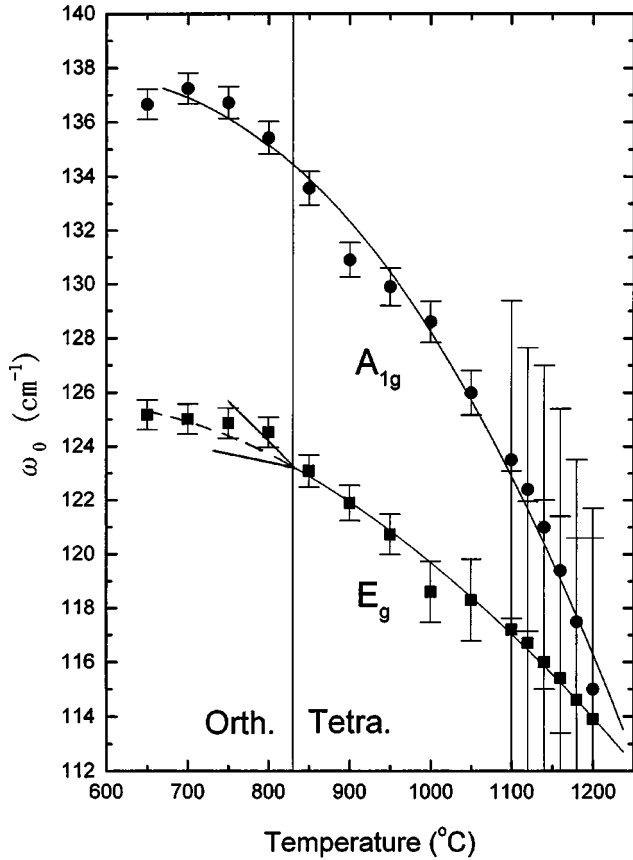


FIG. 3. Temperature dependence of the soft phonon modes in  $\text{SrZrO}_3$ . The dashed line in the orthorhombic phase region corresponds to the result of pattern decomposition assuming the tetragonal phase.

ture toward phase-transition temperature [Fig. 4(a)]. The reduced soft mode half-width  $\Gamma/\Gamma(0)$  versus reduced temperature  $t[t=(T_c-T)/T_c]$  satisfies the universal scaling law<sup>11</sup> [Fig. 4(b)]

$$\Gamma(T) = \Gamma(0)t^{-1/2},$$

where a scaling constant  $\Gamma(0)$  is equal to the linewidth at the room temperature. The linewidths of many displacive ferroelectrics such as  $\text{PbTiO}_3$ ,  $\text{GeTe}$ , and  $\text{SrTiO}_3$  follow this law.<sup>11</sup> As the damping constant of the soft modes is small compared with the soft mode frequencies in the entire range of temperature studied, the soft modes remain underdamped.

We can discuss the features of a phase transition as the following four points.

(a) It has been shown that a phase transition in  $\text{SrZrO}_3$  is caused by the condensation of a soft mode of vibration associated with the rotations of the oxygen octahedron in the cubic phase, and that the eigenvectors of this mode  $\langle 100 \rangle$  are the same as the static displacements of the atoms in the lower-symmetry phase.<sup>4</sup>

(b) The static displacements in  $\text{SrZrO}_3$  are attributed to the condensation of a single component of the triply degenerate  $R_{25}$  mode in which the adjacent octahedra along an axis vibrate about the axis in opposite senses.

(c) Since the two lowest-frequency Raman-active  $E_g$  and  $A_{1g}$  modes in the tetragonal ( $I4/mcm$ ) phase originate from the soft, triply degenerate  $R_{25}(F_{2u})$  mode in the cubic

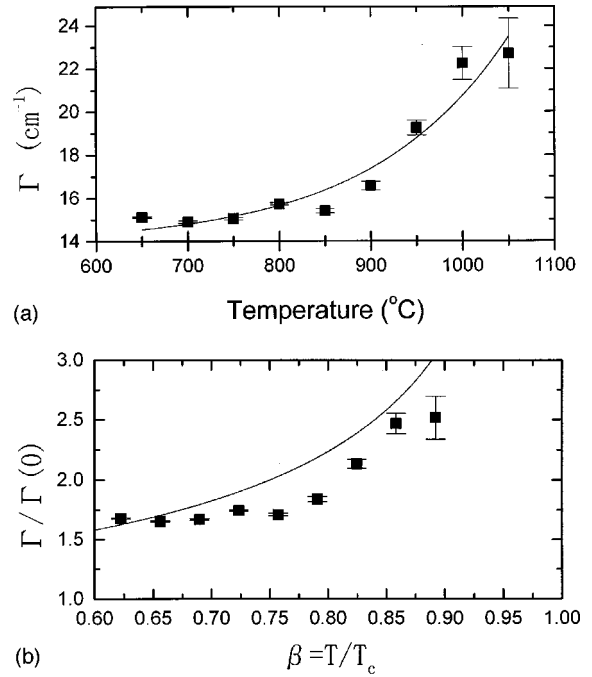


FIG. 4. (a) Temperature dependence of the full width at half maximum of the soft phonon modes in  $\text{SrZrO}_3$ . (b) Reduced soft mode half-width  $\Gamma/\Gamma(0)$  for  $\text{SrZrO}_3$  as a function of reduced temperature. Solid curve represents the equation  $\Gamma/\Gamma(0) = t^{-1/2}$ .

( $Pm\bar{3}m$ ) phase, one might expect the frequencies of both  $E_g$  and  $A_{1g}$  modes to soften as  $T_c - T$  in the tetragonal ( $I4/mcm$ ) phase. This behavior is clearly shown in Fig. 3. The temperature dependence of the  $E_g$  and  $A_{1g}$  branches obeys the Curie-law form ( $\omega^2 \propto T_c - T$ ).

(d) The soft modes remain underdamped, the damping constant of soft modes increased with temperature toward phase-transition temperature satisfying the universal scaling law.<sup>11</sup>

These results are similar to the case of structural phase transition of  $\text{SrTiO}_3$  (Ref. 12) and  $\text{LaAlO}_3$  (Ref. 13).

#### IV. CONCLUDING REMARKS

The neutron powder diffraction data<sup>4</sup> have shown that it was possible to use soft mode  $R_{25}$  picture to explain a phase transition from cubic ( $Pm\bar{3}m$ ) to tetragonal ( $I4/mcm$ ) phase in  $\text{SrZrO}_3$ . However the temperature dependence of soft mode has not been reported yet. A phase transition between cubic ( $Pm\bar{3}m$ ) and tetragonal ( $I4/mcm$ ) phases has been investigated by a new UV Raman spectroscopic system designed to measure the Raman scattering from materials at high temperature, which has enabled us to measure the soft modes in  $\text{SrZrO}_3$  over 1000 °C in this study. We have confirmed that this phase transition is attributed to the condensation of a single component of the triply degenerate  $R_{25}$  mode in which the adjacent octahedra along an axis vibrate about the axis in opposite senses. The soft modes remain underdamped, the damping constant of soft modes increased with temperature toward phase-transition temperature satisfying the universal scaling law.

## ACKNOWLEDGMENTS

The authors would like to express their thanks to Dr. Ryo-suke Shimidzu for his valuable comments. Thanks are also due to Mr. Shigeo Yamamoto for his sample preparation. We

are indebted to Professor Seishi Goto and Professor Koji Ioku of Yamaguchi University for their encouragement. This work was in part supported by the Murata Science Foundation.

---

\*Author to whom correspondence should be addressed. Present address: Department of Advanced Materials Science and Engineering, Faculty of Engineering, Yamaguchi University, Ube, 755-8611, Japan. FAX: +81-836-35-9965. Electronic address: fuji@amse.yamaguchi-u.ac.jp

†Present address: Department of Materials Science and Engineering, Interdisciplinary Graduate School of Science and Engineering, Tokyo Institute of Technology, Yokohama, 226-8502, Japan.

<sup>1</sup>T. Yajima, H. Suzuki, T. Yogo, and H. Iwahara, *Solid State Ionics* **51**, 101 (1992).

<sup>2</sup>A. Ahtee, M. Ahtee, A. M. Glazer, and A. W. Hewat, *Acta Crystallogr., Sect. B: Struct. Crystallogr. Cryst. Chem.* **B32**, 3243 (1976).

<sup>3</sup>L. Carlsson, *Acta Crystallogr.* **23**, 901 (1967).

<sup>4</sup>M. Ahtee, A. M. Glazer, and A. W. Hewat, *Acta Crystallogr., Sect. B: Struct. Crystallogr. Cryst. Chem.* **B34**, 752 (1978).

<sup>5</sup>Y. Zhao and D. J. Weidner, *Phys. Chem. Miner.* **18**, 294 (1991).

<sup>6</sup>D. Ligny and P. Richet, *Phys. Rev. B* **53**, 3013 (1996).

<sup>7</sup>K. S. Aleksandrov, *Ferroelectrics* **16**, 801 (1976).

<sup>8</sup>K. S. Aleksandrov, *Ferroelectrics* **20**, 61 (1978).

<sup>9</sup>M. Yashima, M. Kakihana, R. Shimidzu, H. Fujimori, and M. Yoshimura, *Appl. Spectrosc.* **51**, 1224 (1997).

<sup>10</sup>M. Kakihana, *J. Sol-Gel Sci. Technol.* **6**, 7 (1996).

<sup>11</sup>J. F. Scott and J. A. Sanjurjo, *Solid State Commun.* **58**, 687 (1986).

<sup>12</sup>P. A. Fleury, J. F. Scott, and J. M. Worlock, *Phys. Rev. Lett.* **21**, 16 (1968).

<sup>13</sup>J. F. Scott, *Phys. Rev.* **183**, 823 (1969).